ELSEVIER

Thermochimica Acta 330 (1999) 45–54

thermochimica acta

Temperature modulated differential scanning calorimetry (TMDSC) in the region of phase transitions. Part 1: theoretical considerations

G.W.H. Höhne

Universität Ulm, Sektion für Kalorimetrie, Albert-Einsteinallee 11, D-89081 Ulm, Germany

Received 3 November 1998; accepted 23 December 1998

Abstract

For temperature modulated differential scanning calorimetry (TMDSC) a simple model, the low pass filter, is presented which allows to see and calculate the influence of heat transfer into the sample on magnitude and phase shift of the modulated part of the measured heat flow rate and the heat capacity determined from it. A formula is given which enables to correct the measured magnitude of the periodic heat flow rate function and the calculated heat capacity in dependence on the thermal resistance and heat capacity of the sample. The correction becomes very important in regions where the heat capacity changes considerably as in the melting region. The approach is successfully tested with model substances with well-known excess heat capacity in the transition region. © 1999 Elsevier Science B.V. All rights reserved.

Keywords: DSC; Temperature modulated DSC; Phase transition; Heat transfer; Heat capacity

1. Introduction

Temperature modulated differential scanning calorimetry (TMDSC) offers against normal DSC additional possibilities to get information about dynamic (i.e. time-dependent) processes inside the sample. This is especially of importance in polymer research, as macromolecules need time to rearrange at transitions of all kind. Fortunately the time constant of such processes falls often into the time window covered by common DSC equipment. The TMDSC method has already proved its worth in the case of the glass transition of amorphous polymers. For this region many papers have been published, the behavior of the apparatus seems to be well understood and additional information about the glass process could be extracted from TMDSC measurements.

For the melting region the situation is, however, different and interpretation of respective measurements (which of course have been done) seems, friendly speaking, to be risky. Too little is known yet about the artifacts produced by the apparatus itself and not by the sample in question. This paper aims at making a contribution to better understand the behavior of the TMDSC in the melting region. This is done by means of very simple model considerations which in a second step have been proved experimentally using samples which certainly do not show time-dependent processes.

The model of choice is that of electrical analogy, which has proved its worth in DTA and DSC analysis since decades [1]. From the physical point of view the transport of energy (heat flow) is based on the same type of equations as is the transport of charge (current), so the knowledge from theory of electricity (in

0040-6031/99/$ – see front matter
PII: S0040-6031(99)00039-8

particular alternating current (a.c.) theory) can easily be transferred to heat transport problems. The advantage of looking on electrical networks rather than on often complex heat conducting solid objects is that there are a lot of powerful tools from electrical line network and transfer theory available and the wheel must not be invented once more.

The ''dictionary'' of the two languages of the same transport physics reads as follows:

Heat transport	Charge transport
Heat Q	Charge Q
Heat flow rate Φ	Current i
Temperature T	Voltage (against some zero reference) U
Heat resistance R_{th}	Resistance R
Heat conductivity λ	Conductance L
Heat capacity C_p	Capacitance C

The DSC is built from different mechanical parts, which in principal have a certain heat conductivity and a heat capacity each. A contact area between different parts acts as an additional heat resistance. In addition there is often sophisticated electronics which amplifies the voltages from the sensors resulting in the measured signal transferred to the computer. This way a DSC, no matter how complicated it is, can be dissected into a network of simple mechanical elements – which can be translated into an electrical network of capacitances and resistors, see e.g. [1,2] – and the hopefully linear electronics. There is no limit for the number of elements in such a network. To get the properties of it, a system of almost the same number of linear differential equations must be solved which in principal is possible, even for complex modern equipment, thanks to modern computers. Nevertheless we shall, in what follows, restrict ourselves to very simple models which are absolutely sufficient to learn about the principle behind heat transfer to the sample in case of modulated DSC.

In this case the network describing the DSC in question has one input (the temperature program) and one output (the heat flow rate into the sample calculated from the differential temperature or directly measured as differential heat flow rate). It is often sufficient to look at the so-called ''transfer function'' (a complex function in frequency space, see below) to describe the ''black box'' containing the network in question. The transfer function is closely connected with the ''step response'' or ''impulse response'' functions (in time–space) via Fourier transform. It will go beyond the scope of this paper to derive all details of the features of these functions, the interested reader is referred to textbooks of transfer theory or, more basically, of a.c. electricity physics.

2. Simple models for DSCs

2.1. The low pass filter

The easiest model for, say, a sample inside the sample pan which has a certain thermal resistance R_{th} and a certain heat capacity C_p is a RC element (Fig. 1). The input voltage U_i of the electrical circuit stands for the temperature of the pan support T_S and the output voltage U_o stands for the (mean) temperature of the sample itself T_{sample}. The transfer function $P(\omega)$ is defined as the quotient of the output function $U_o(\omega)$ over the input function $U_i(\omega)$ which for the network of Fig. 1 can easily be found from the respective resistances R and R_C (the a.c. resistance of C):

$$P(\omega) = \frac{U_o(\omega)}{U_i(\omega)} = \frac{R_C}{R + R_C} = \frac{1/i\omega C}{R + 1/i\omega C} = \frac{1}{1 + i\omega RC} = \frac{1}{1 + \omega^2 R^2 C^2} - i\frac{\omega RC}{1 + \omega^2 R^2 C^2}. \quad (1)$$

This is the complex transfer function of the electrical circuit. The transfer function of the thermal behavior of the sample is got by changing R to R_{th}, C to C_p and the voltages to the respective temperatures. For DSC the transfer function plays the role of a correction factor for heat flow rate and C_p function,

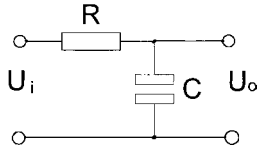

Fig. 1. Circuit representing a low pass filter.

respectively. This way we get the magnitude (amplitude)

$$|P(\omega)| = \sqrt{(\mathrm{Re}\,P(\omega))^2 + (\mathrm{Im}\,P(\omega))^2} = \frac{1}{\sqrt{1+\omega^2 R_{\mathrm{th}}^2 C_p^2}} = \left|\frac{T_{\mathrm{sample}}}{T_{\mathrm{S}}}\right|. \quad (2)$$

and the phase angle of the transfer function in terms of thermal quantities:

$$\arg(P(\omega)) = \tan^{-1}\frac{\mathrm{Im}\,P(\omega)}{\mathrm{Re}\,P(\omega)} = \tan^{-1}|-\omega R_{\mathrm{th}} C_p| = \phi(\omega). \quad (3)$$

Having the fact in mind that the heat flow rate signal can only be behind the temperature signal in time because it is caused by the latter, we can neglect the sign in Eq. (3) and define the phase shift of the periodic heat flow rate function in TMDSCs as always positive.

As an example in Fig. 2 the magnitude of such a sample transfer function is plotted for three different cases representing the respective values of realistic samples: (a) a 7.8 mg sapphire disc, (b) a 9 mg polystyrene disc and (c) a 280 mg copper disk, respectively. Fig. 3 represents the log–log plot (the so-called ''Bode plot'') of this transfer function. The product $R_{\mathrm{th}}C_{\mathrm{p}}=\tau$ has the dimension of a time which determines the temperature relaxation behavior of the sample in its pan. It can be determined from the measured transfer function (see Eqs. (2) and (4)), namely by extrapolating the asymptotes from very low (a horizontal line) and very high frequencies (a line with slope=−1) in the Bode plot (see Fig. 3). The intersection point ω_0 (the ''corner frequency'' of the low pass filter) gives the reciprocal τ and thus even the effective R_{th} for known heat capacity of the sample C_p.

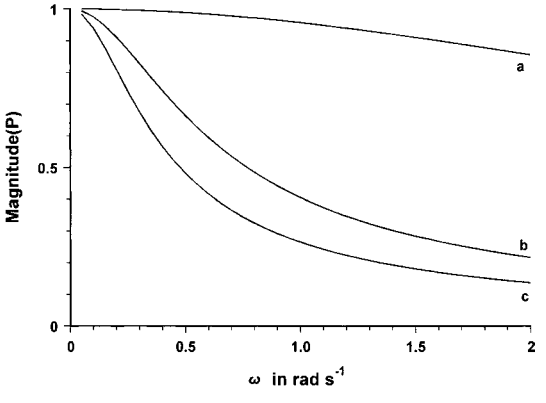

Fig. 2. Magnitude of the transfer function of the low pass filter model for: (a) a sapphire disc (R_{th}=0.04 K mW^{-1}, C=7.2 mJ K^{-1}, τ=0.30 s); (b) a polystyrene disc (R_{th}=0.18 K mW^{-1}, C=12.5 mJ K^{-1}, τ=2.25 s); (c) a copper disc (R_{th}=0.033 K mW^{-1}, C=110 mJ K^{-1}, τ=3.63 s) in usual sample pans.

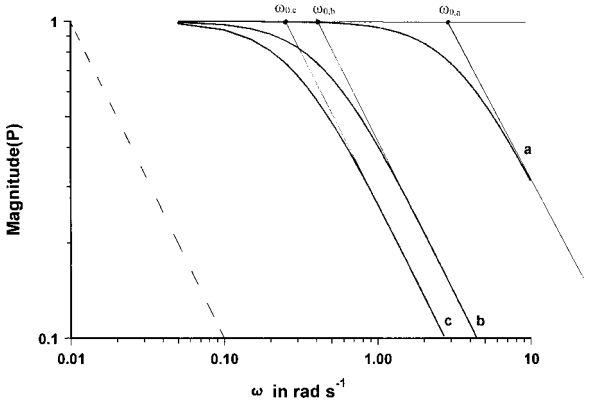

Fig. 3. Bode plot (magnitude) of the transfer function of Fig. 2 with construction of the corner frequencies. The dashed line indicate the slope of −1.

From Eq. (2) we get

$$|T_{\mathrm{sample}}| = \frac{1}{\sqrt{1+\omega^2 R_{\mathrm{th}}^2 C_p^2}}|T_{\mathrm{S}}|. \quad (4)$$

With other words the (mean) sample temperature magnitude (amplitude) is always lower than that of the pan support which is the measured (and controlled) quantity. If we consider the TMDSC itself (i.e. the temperature probe) well calibrated, Eq. (4) enables us to correct our measured results due to the limited heat transport into the respective sample.

It is clear that the product of R_{th} and C_p determines the transfer behavior (see Figs. 2 and 3). Both the polystyrene sample with low heat capacity but high heat resistance and the copper sample with low heat resistance but high heat capacity show a fast decreasing magnitude of the transfer function with ω, whereas that of the sapphire sample does not change so much because both R_{th} and C_p are rather small.

Let us try to apply our knowledge from this simple model to heat capacity measurement with TMDSC. The oscillating part of the temperature program

reads e.g.

$$\tilde{T}_S(t) = T_A \sin \omega t, \tag{5}$$

where $T_A = |\tilde{T}_S|$ is the temperature amplitude of the sample thermometer which often controls the temperature program. Then, for very symmetrical and ideal thermal conditions, the measured differential heat flow rate (i.e. the heat flow rate into the sample with heat capacity C_p) is simply given by

$$\tilde{\Phi}(t) = C_p \frac{d\tilde{T}}{dt} = C_p \cdot T_A \cdot \omega \cdot \cos \omega t = \Phi_A \cos \omega t, \tag{6}$$

from which the heat capacity of the sample is calculated:

$$C_p = \frac{\Phi_A}{T_A \cdot \omega}. \tag{7}$$

But this simple formula is only true for frequencies low enough to allow the sample temperature to follow the program temperature totally, otherwise the (always lower) sample temperature amplitude – instead of the program temperature Eq. (5) – must be used in Eqs. (6) and (7) and we get with Eq. (4):

$$C_p = \frac{\Phi_A}{T_A \cdot \omega} \sqrt{1 + \omega^2 R_{th}^2 C_p^2}. \tag{8a}$$

Strictly speaking the C_p's on both sides are not the same because of unavoidable asymmetries between reference and sample side. Both are ''apparent'' heat capacities as ''seen'' from the thermometer on the one hand and from the bottom of the sample pan on the other hand. However, the difference is not very large and within the framework of this model discussion we decide both quantities to render the sample heat capacity, taking ideal symmetry of the DSC into account. This way we may solve Eq. (8a) for C_p:

$$C_p = \frac{\Phi_A}{\omega \sqrt{T_A^2 - R_{th}^2 \Phi_A^2}}. \tag{8b}$$

The correction term (the square root in Eq. (8a)) can be neglected if $\omega^2 R_{th}^2 C_p^2 \ll 1$. To decide on this, we have to know something about the apparent thermal resistance R_{th}, which includes both the heat transfer to and the heat conduction inside the sample. The apparent thermal resistance can be determined from the ascending slope ($d\Phi/dT = 1/R_{th}$) of a peak from a first order transition [2] of a sample with the same thermal properties which can be measured in normal DSC mode, or – with TMDSC – from the heat flow rate amplitude during phase transition. To see the latter, we rearrange Eq. (8a):

$$\Phi_A = T_A \frac{\omega \cdot C_p}{\sqrt{1 + \omega^2 R_{th}^2 C_p^2}}. \tag{9}$$

During a first order phase transition the apparent (excess) heat capacity of the sample becomes infinite and the number 1 in the denominator can be neglected against the second term and we get

$$\Phi_A \cong \frac{T_A}{R_{th}}. \tag{10}$$

This is the maximum possible magnitude of the periodic heat flow rate for a given temperature amplitude in a TMDSC. This case may occur during first order phase transitions (see Section 3.1).

For those who are in need of the phase shift for evaluation as well, we stress that there is even a huge influence of the sample properties R_{th} and C_p on the measured phase shift which can be corrected in a similar way by using Eq. (3). This correction is straightforward beside the problems arising from the periodicity of the $\tan^{-1}$(arc tan) function.

What do we learn from these considerations for TMDSC measurements in the phase transition region: as the apparent (effective) heat capacity changes considerably during phase transitions, the heat flow rate magnitude is not proportional to the heat capacity any more. Within the framework of this simple model, and taking total symmetry of the TMDSC for granted, formula Eq. (9) is valid. The true excess heat capacity of, say, polymer melting may be calculated from the measured heat flow rate magnitude by means of Eq. (8a) or Eq. (8b). For narrow first order transitions this is meaningless, as the magnitude does not contain any information from the heat capacity anymore. Even outside the melting region where C_p is almost constant, the correction factor is usually different from unity and should be determined experimentally.

2.2. Low pass filter networks

The low pass filter model is even helpful to understand the properties of the total equipment i.e. DSC

and sample due to heat transport influence on the measurement. In a first approximation the heat is transported along a one-dimensional pathway which can be modeled by a series of *RC* elements. Say, for instance for the sample side, one from the oven to the sample (or control) thermometer, one from that thermometer to the sample support (the pan) and one from there to the inner side of the sample. All these *RC* elements have different apparent heat resistances and heat capacities, which of course are unknown but (for the apparatus part) almost constant. They can be determined from the measured transfer function, if necessary, as will be shown later.

From transfer theory it is well known that for transfer elements connected in series the total transfer function is the product of those from the elements. In other words, the amplitudes have to be multiplied, whereas the phases connect additive. This way the total correction, concerning the heat transfer, of the heat flow rate function can be deduced from Eq. (9) with different $\tau = R_{\mathrm{th}} C_p$ for the *RC* elements in question

$$\Phi_{\mathrm{A}} = T_{\mathrm{A}} \omega C_p \prod_{i=1}^{n} \frac{1}{\sqrt{1+\omega^2 \tau_i^2}}$$

$$\text{or} \quad \log \frac{\Phi_{\mathrm{A}}}{T_{\mathrm{A}} \omega C_p} = \sum_{i=1}^{n} \log \frac{1}{\sqrt{1+\omega^2 \tau_i^2}}. \qquad (11)$$

If we measure the heat flow rate magnitude Φ_{A} depending on ω for different heat capacities C_p and plot $\log(\Phi_{\mathrm{A}}/(\mathrm{T_A}\ \omega\ C_{\mathrm{p}}))$ against $\log\ \omega$ (“Bode plot”) we get curves which starts horizontally and bends more and more down. If a sample is chosen with low heat capacity and low thermal resistance its transfer function will not influence the measurements within the available frequency region very much and we get the transfer function of the apparatus itself. From the slope of the asymptote in the double logarithmic plot it is possible to determine the number of different effective *RC* elements. One *RC* element will give a slope of -1 at higher frequencies (see Fig. 3), two *RC* elements in series will give a slope of -2 and so on. Determining the intersections of the asymptotes (as in Fig. 3), starting at the lowest frequencies, and subtracting the respective curve from the measured one will give all respective time constants for those who are interested.

For practice it is sufficient to take the total transfer function for correction of apparative heat transfer influences on the measured signal. This function itself, if determined correct, should not depend on sample parameters. The sample behavior can then be easily included by adding both Bode plots. Of course the respective apparative correction must be done first if information from sample influences must be deduced.

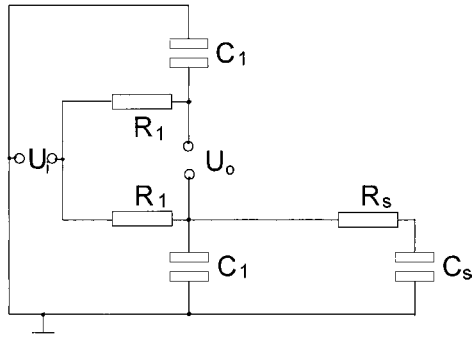

Fig. 4. Circuit representing the simplest model for a DSC with sample.

As an simple example for modeling the total TMDSC, the simplest possible network of Fig. 4 has been constructed. The transfer function for this model is again defined as the quotient of the output voltage (i.e. the ΔT signal of the DSC) over the input voltage (i.e. the temperature of the oven). It can be calculated straightforward in a similar way as that of the low pass filter (Section 2.1) using the laws of electricity in particular Kirchhoff’s laws (see [2,3]):

$$\frac{U_{\mathrm{o}}}{U_{\mathrm{i}}} = \frac{1}{1+\mathrm{i}\omega R_1 C_1} - \frac{1}{1+\mathrm{i}\omega R_1 C_1 + \omega R_1\, C_{\mathrm{S}}/(\omega R_{\mathrm{S}} C_{\mathrm{S}} - \mathrm{i})}. \qquad (12)$$

This is the difference between the transfer functions of a single low pass and that of two low pass in series representing the reference side and the sample side of a differential calorimeter, respectively. The quantities R_1 and C_1 characterize the apparent thermal resistance and the apparent heat capacity of the heat flow pathway from the oven to the pans, which are thought to be the same on sample and reference side. R_{S} and C_{S} symbolize similar quantities for the sample itself. The (normalized) magnitude of this function (Eq. (12)) is calculated with MAPLE mathematics software and plotted in Fig. 5 after inserting parameters chosen to give the best fit to real measurements with a

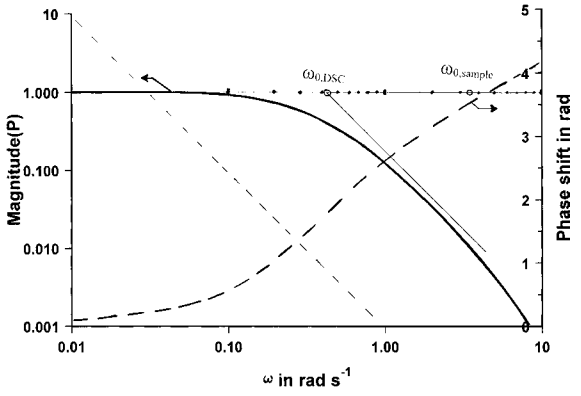

Fig. 5. Bode plot of magnitude and phase of the transfer function of the DSC model (Fig. 4) (with thermal quantities: R_1=0.115 K mW^{-1}, C_1=20 mJ K^{-1}, τ_1=2.3 s, R_S=0.04 K mW^{-1}, C_S=7.2 mJ K^{-1}, τ_S=0.30 s).

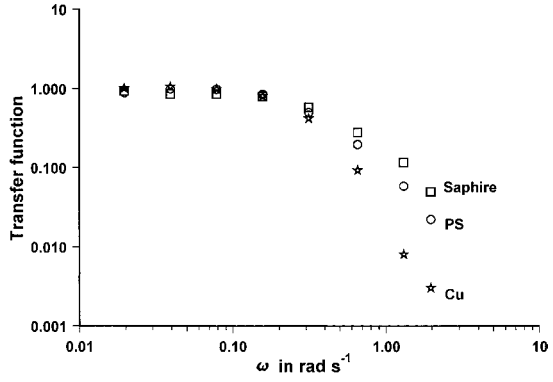

Fig. 6. Bode plot (magnitude) of the transfer function (Φ_A/($T_A\,\omega\,C_p$)) of a DSC7 in isothermal modulation mode (T_A=23 mK) measured at eight frequencies with three different samples (for properties see Fig. 2).

sapphire disc. The typical low pass filter behavior is visible even for this more complex network. The slope for higher frequencies is about −2 in this ''Bode plot''. The intersection point of the asymptotes (corner frequency) is ω_0=0.45 rad s^{-1} which yields a time constant of 2.2 s which fits with the chosen parameters R_1C_1=0.115 K mW^{-1}×20 J K^{-1}=2.3 s. The corner frequency which belongs to the low pass element characterizing the sample in this model (ω_0=3.45 rad s^{-1} for the parameters used: R_SC_S= 0.29 s) is got if we extrapolate the asymptote at large frequencies.

2.3. Measurements supporting the model calculations

To test the model calculations measurements with a real TMDSC (DSC7, Perkin-Elmer, with self-made modulation possibility[1]) and evaluation with phase sensitive rectification method [4] were done, using three different samples (the same as used for the calculations of Fig. 3). In Fig. 6 the measured magnitude of the total transfer function of calorimeter with these samples at different frequencies is given in the form of a ''Bode plot''. In this case the transfer function $P(\omega)$ is defined by the quotient of the measured heat capacity (the ''output'' of the measurement) and the true heat capacity (the ''input'' of the measurement) of the sample. The former is calculated using uncorrected Eq. (7), the latter is taken from literature. As can be seen, the overall shape of the curves looks like the calculated one (Fig. 5). Even the influence of the different samples on the curvature at frequencies ω>0.1 rad s^{-1} is clearly visible. This is clear from the different sample low pass behavior (see Fig. 3), which comes in at those frequencies and the fact that the overall ''Bode plot'' is the sum of the ''Bode plots'' of the TMDSC and the sample in question.

As it looks like this TMDSC (though a power compensated one) seems to follow the very simple low pass filter model rather well. Obviously the power compensation electronics has no essential influence within the frequency window used. This makes us optimistic for the validity of the following considerations.

2.4. Remark on the damping effect of temperature waves in solids

In heat conducting materials a periodic temperature change on one side of the sample generates a temperature wave which proceeds through the sample in time. This wave is, however, very damped, in other words the amplitude decreases exponentially and the effective penetration length of the temperature wave (i.e. the distance where the amplitude is reduced to 1/e,

[1]By adding a sinusoidal voltage from a precision function generator to the program voltage of the electronic controller.

see textbooks of solid state physics) reads

$$\delta = \sqrt{\frac{2\alpha}{\omega}} \quad \text{with} \quad \alpha = \frac{\lambda}{\rho c_p}, \tag{13}$$

where α is the thermal diffusivity, λ the thermal conductivity, ρ the density and c_p is the specific heat capacity. For the frequencies of TMDSC this length is in cm range for metals like copper, but below 1 mm for polymers. The consequence of this low penetration length for our considerations is that for the modulated part of the temperature we have an exponential temperature decrease inside the sample. In other words, the real amplitude decreases exponentially from the contact surface towards the center of the sample. And this is already an essential effect for organic or polymer samples of, say, half a millimeter thickness. We have to draw conclusion that the sample temperature amplitude got from the correction formula of our simple low pass filter model (Eq. (4)) is in fact an exponential average value, which for thicker samples represent the reality only very roughly. The same is true for the subsequent calculated heat capacity.

3. TMDSC behavior in the phase transition region

In what follows different measurements with our TMDSC characterized above are presented. To avoid unnecessary complications we restrict ourselves to the heat flow rate functions as evaluated from the measured heat flow rate without any correction. The aim of this section is to deduce the influence of the sample on the measured quantities in the transition region in principle and see how the latter are falsified by the low pass filter behavior.

3.1. First order phase transition of a pure substance

For first order phase transitions the enthalpy passes through a step-like change at the fixed transition temperature. From that it follows that the heat capacity (the derivative of the enthalpy) becomes Dirac shaped (i.e. infinite) at transition temperature. From the considerations in Section 2.1, Eq. (10) should be valid in the transition region, in other words, within the region of the melting peak the magnitude of the periodic heat flow rate should increase to the maximum value

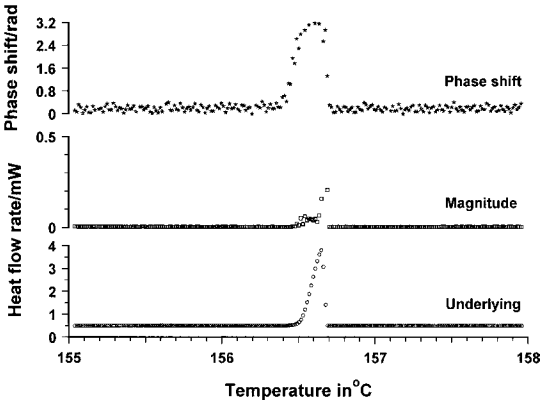

Fig. 7. TMDSC run in only heating mode of indium in the melting region (m=6.5 mg, ω=0.39 rad s^{-1}, period=16 s, T_A=2.3 mK, underlying heating rate 0.1 K min^{-1}).

(saturation) which is determined by the thermal resistance and the temperature amplitude. As mentioned before, this way the apparent thermal resistance of the sample can be determined: $R_{th}=T_A/\Phi_A$. From Eq. (3) the phase shift coming from the sample low pass filter should be $\pi/2$. In the other low pass filter characterizing the heat flow pathway in the DSC the big heat flow into the sample causes another $\pi/2$ phase shift. Remembering that phases behave additive for serial low pass filters, the total phase should jump by π in the melting region.

In Figs. 7 and 8 the experimental results for the melting of indium for two different temperature amplitudes are given. The amplitudes are chosen that way to give a temperature program in only heating or heating–cooling mode, respectively. The behavior of the magnitude of the periodic heat flow rate as well as the phase shift is as expected. The effective thermal resistance of that indium sample is calculated from Eq. (10) R_{th}=48 K W^{-1} which fits to the value 35 K W^{-1} got from the slope of the melting peak from a conventional DSC run, which is reflected in the underlying curve even got from TMDSC measurements in the usual way. For precise evaluation we have to have in mind that again the program temperature amplitude, used for calculation, is somewhat higher than the amplitude at the bottom of the pan. The time constant of the sample (outside the melting region) can be calculated from the thermal resistance and the heat capacity of the sample: $\tau=R_{th}C_p$=0.2 s which together with the used frequency ω=0.39 rad s^{-1}

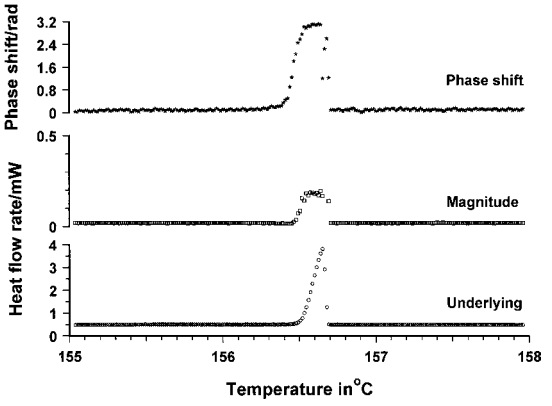

Fig. 8. TMDSC run in heating–cooling mode of indium in the melting region (m=6.5 mg, ω=0.39 rad s^{-1}, period=16 s, T_A=9.2 mK, underlying heating rate 0.1 K min^{-1}).

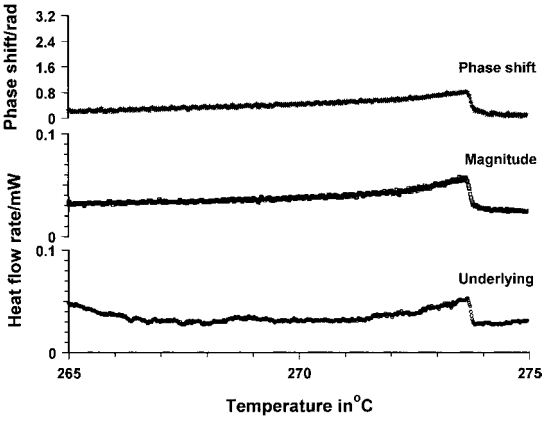

Fig. 9. TMDSC run in heating–cooling mode of $NaNO_3$ in the transition region (m=4.8 mg, ω=0.39 rad s^{-1}, period=16 s, T_A=9.2 mK, underlying heating rate 0.1 K min^{-1}).

results in a value of 0.006 for the second term of the square root in the correction formula Eq. (4) which can be neglected against 1, so outside the melting region there is no correction needed.

3.2. Second order phase transitions

Second order phase transitions show no step-like enthalpy change at a certain fixed temperature but a continuous increase within a definite temperature interval. The respective derivative, the heat capacity function, looks often like a capital Greek lambda (Λ) i.e. increases with temperature with increasing slope and drops suddenly down to the low temperature value again. The temperature at maximum is taken as the transition temperature.

Such a C_p anomaly (clearly without any relaxation or other time-dependent processes) is very suitable to test the TMDSC and our formulae.

In Fig. 9 the results from measurements of the second order transition of $NaNO_3$ at 274°C are shown. The Λ-transition is clearly visible both in the underlying and in the magnitude curve of the heat flow rate. As the heat capacity does not change very much (about a factor of 2 within the first 90% of the peak) and the thermal resistance seems to be rather low, the denominator of Eq. (9) equals 1 and can be omitted in this case. This is one example, where it is not necessary to correct for sample low pass behavior, at least for our special TMDSC and this transition. The magnitude of the modulated part of the signal is, even during the transition, proportional to the heat capacity.

The phase shift is rather small during the second order transition (Fig. 9) and obviously proportional to the heat capacity as well. This is in accordance with Eq. (3), as for small heat capacity changes, the $\tan^{-1}$ function can be replaced by its argument.

To sum up, for second order phase transitions and other events with rather small heat capacity changes the underlying magnitude and phase shift curves, respectively, reflect the $C_p(T)$ function and may be used to determine it. Determination from the magnitude curve is, however, most precise. An eventual correction, which is due to low pass filter behavior of the sample itself, can be done using Eq. (8a) or Eq. (8b). There is no additional information in the phase shift curve.

3.3. Melting with continuous enthalpy function

Looking for a system with a broad melting region, as known from polymers, but without any measurable time dependence, we chose an impure alkane ($C_{33}H_{68}$). From alkanes it is well known that melting is an almost instantaneous process. Even the thermodynamics of alkane mixtures (as in an impure alkane) is well known, they behave eutectic if the chain length is not to narrow. Consequently, the melting peak of such an impure alkane should start immediately after the eutectic temperature and end somewhat below the

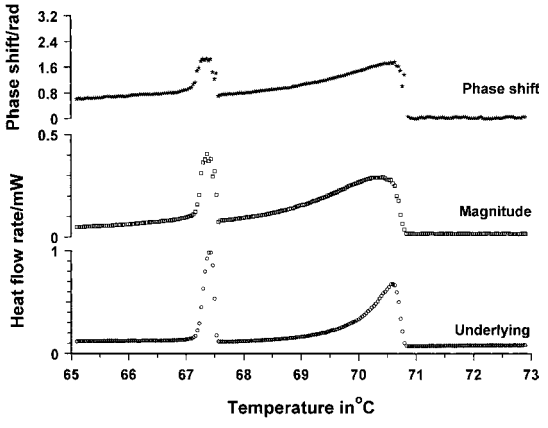

Fig. 10. TMDSC run in heating–cooling mode of an impure $C_{33}H_{68}$ in the melting region (m=2.25 mg, ω=0.16 rad s^{-1}, period=40 s, T_A=23 mK, underlying heating rate 0.1 K min^{-1}).

melting temperature of the main component ($C_{33}H_{68}$). The shape of the heat capacity function is again the derivative of the enthalpy function which can be calculated with well established thermodynamic formulas. For our purposes only the shape of the $C_p(T)$ function is of interest which again is Λ-shaped and has a width of about 3 K. The exact course of it depends, however, on the components of the mixture or, in our case, the impurities in question, but this is not of interest here.

In Fig. 10 the underlying heat flow rate curve as well as the magnitude and the phase shift of the modulated part of the respective TMDSC signal is plotted. Comparing the underlying heat flow rate curve with the magnitude curve we see that the curvature of the magnitude curve is significantly lower than that of the underlying curve. Obviously there is an increasing ''damping'' of the heat flow magnitude with increasing peak height. The reason for that is

1. the larger apparent thermal resistance of the sample R_{th}=60 K W^{-1} and
2. the large increase of excess heat capacity within the peak (more than 50 times!).

The time constant outside the melting region is $\tau=R_{th}C_p$=0.3 s, a value which together with the frequency ω=0.39 rad s^{-1} yield a value of 0.1 for the second term under the square root (Eqs. (4) and (8a)), which cannot be neglected for precise measurements. Its value increases more and more along the melting peak and gets larger than 5 at peak maximum. From this it follows that we have to take a rapid increasing correction factor into account and at peak maximum the measured magnitude of the periodic heat flow rate must be multiplied with a factor of about 3 to give the exact C_p function. This can be seen in Fig. 10, the magnitude curve, compared with the underlying curve, becomes more and more flat approaching the maximum of the melting peak, because of the increasing denominator. Looking at the first order solid–solid transition peak at 67°C – where our considerations of Section 3.1 are valid – we can see the maximum possible magnitude of the periodic heat flow rate for this sample at 0.38 mW. Obviously the magnitude at the maximum of the melting region (0.3 mW) is approaching this limit. If we would include the correction factor we would get a magnitude curve looking like the underlying curve in the melting region, both of them being almost proportional to the heat capacity curve.

To test the validity of our considerations furthermore we have done quasi-isothermal measurements on the same sample with the same temperature amplitude. In Fig. 11 these results have been added to the magnitude curve of Fig. 10 for comparison. In the melting region and outside the transitions the measuring points coincide with the magnitude curve of the scanning mode, this result supports

1. our assumption that the melting curve can be described by an excess heat capacity function and

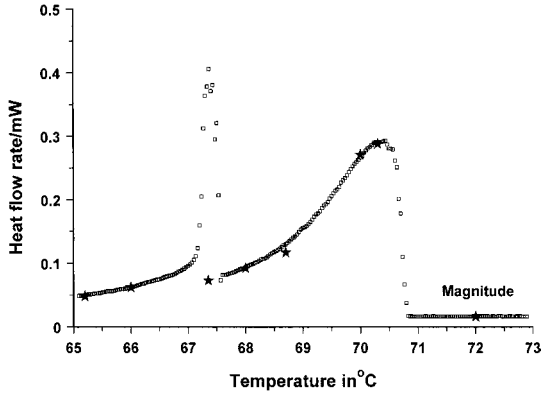

Fig. 11. Magnitude curve from Fig. 10 together with results from measurements in quasi-isothermal mode with the same temperature amplitude.

2. the idea of low pass filter behavior to be even valid for the quasi-isothermal mode of modulation.

The one measuring point within the first order solid–solid phase transition reproduce the static heat capacity of the sample (the base line) at that temperature. Even that result is as expected for ''sharp'' first order phase transitions.

4. Conclusions

The experiments have shown that the simple low pass filter model is a suitable approach to describe the TMDSC in a region where the apparent heat capacity (or the thermal resistance) changes are considerable. As a consequence the sample temperature modulation amplitude is a function of the heat capacity of the sample as well as that of the apparent thermal resistance. The measured magnitude of the modulated part of the heat flow rate is never strictly proportional to the heat capacity function but a correction must be included. This correction can be approximated by

$$\Phi_{\mathrm{A,corr}} = \Phi_{\mathrm{A,meas}} \cdot \sqrt{1 + \omega^2 R_{\mathrm{th}}^2 C_p^2}. \qquad (14)$$

Normally C_p is the desired result from TMDSC measurements and Eq. (8a) or Eq. (8b) is used to calculate the corrected C_p directly from the measured heat flow rate magnitude. In this case the corrected heat flow rate itself is of no interest. However, R_{th} and C_p are not known exactly, but it is possible to get some approximate values for the sample in question. For $C_p(T)$ in Eqs. (14) and (8a) the underlying heat flow rate divided by the (underlying) heating rate can be used as an zeroth approximation and R_{th} can be determined from the slope of a first order transition of the sample in question. If such a thing does not exist (e.g. for polymers) one could take the respective result from measurements with substances of similar thermal conductivity properties. This way pure alkanes may serve as substitute for, say, polyethylene. Of course it is also possible to determine the product $R_{\mathrm{th}}C_p$ experimentally for a certain polymer by comparing the measured heat capacity (outside of transition regions) for different frequencies ω (as many as possible) with the value from literature (e.g. from the ATHAS data bank [5]) and making a least square fit by means of the correction function. It is clear that such a correction is only a very approximate one, but such a correction is in every case better than to calculate an excess heat capacity in a transition region without any correction of the measured magnitude of the periodic heat flow rate.

Knowing the influence of the heat transfer on TMDSC results enables the scientist to decide whether there is some additional (time-dependent) process in the sample or whether the measurements mirrors only the pure excess heat capacity in the transition region. Examples will be presented in the second part of this paper [6]

Last but not the least it should be mentioned that similar considerations can be done for the influence of the sample on phase shift in the melting region. The calculations and corrections are, however, not so easy but the low pass filter model is successful even in this case [7].

Acknowledgements

The author would like to thank all participants of the Fifth Lähnwitz seminar who contributed by intensive discussion at the poster in question that the ideas became more clarified.

References

[1] F.W. Wilburn, J.R. Hesford, J.R. Flower, Anal. Chem. 40(4) (1968) 777–788.
[2] G.W.H. Höhne, W. Hemminger, H.J. Flammersheim, Differential Scanning Calorimetry, Springer, Berlin, 1996.
[3] G.W.H. Höhne, Thermochim. Acta 69 (1983) 175–197.
[4] G.W.H. Höhne, Thermochim. Acta 304/305 (1997) 209–218.
[5] B. Wunderlich et al., ATHAS databank, see www: http://funnelweb.utcc.utk.edu/∼athas/databank.
[6] G.W.H. Höhne, Thermochim. Acta 330 (1999) 93–99.
[7] G.W.H. Höhne, M. Merzlyakov, C. Schick, in preparation.